Nuclear Physics B309 (1988) 221–258
North-Holland, Amsterdam

DELAYED UNITARITY CANCELLATION AND HEAVY PARTICLE EFFECTS IN $e^+e^- \to W^+W^-$

Changrim AHN and Michael E. PESKIN[1]

Stanford Linear Accelerator Center, Stanford University, Stanford, CA 94309, USA

Bryan W. LYNN[2] and Stephen SELIPSKY[3]

Department of Physics, Stanford University, Stanford, CA 94309, USA

Received 11 May 1988

We examine one-loop radiative corrections to $e^+e^- \to W^+W^-$ in the standard model with one Higgs doublet, concentrating on the effects of very heavy fermions. These disturb the delicate unitarity cancellation between s- and t-channel diagrams, raising the cross section even well below the fermion threshold and giving a clear experimental signature for the heavy sector.

1. Introduction

Radiative corrections allow us to probe the high-energy world with comparatively low-energy experiments. Because any intermediate state allowed by symmetry, however heavy, can appear as a quantum fluctuation, precision experiments which isolate radiative corrections can probe for particles with masses much higher than the experimental energy scale. The most sensitive of such experiments are those which involve flavor mixing, such as the measurement of the K_L–K_S mass difference. However, even quantities which entail no special flavor violation, such as the muon ($g-2$), can yield important information on heavy states. Now that we are entering the era of experiments on the properties of the weak vector bosons, it is interesting to think of precision experiments which might be carried out on these new fundamental particles. Such experiments would necessarily be done at energies of 100 GeV, or even much higher; still, extending the reach of the available machine

[1] Work supported by the Department of Energy, contract DE-AC03-76SF00515.
[2] Work supported by the National Science Foundation, contract NSF-PHY-86-12280.
[3] Work supported by a National Science Foundation Graduate Fellowship.

0550-3213/88/$03.50

energy by measurements sensitive to the radiative corrections is an attractive possibility.

Two important experiments of this type which have been discussed extensively in the literature are the measurements of the W-boson mass [1–5] and the polarization asymmetry for fermion pair production at the Z^0 resonance [4–6]. Both of these experiments are difficult, requiring large statistical samples and methods which cancel systematic errors below the 1% level. Yet in both cases the influence of new heavy states is larger than one has a right to expect. Naively, one would predict that electroweak radiative corrections due to new particles of mass M would affect the masses and couplings of the weak bosons by terms of order α/π, times a factor m_W^2/M^2 representing the Appelquist–Carazzone decoupling [7]. However, the Appelquist–Carazzone theorem does not apply to theories with chiral gauge couplings or large mass splittings within gauge multiplets, and indeed one finds by explicit calculations both terms with no suppression for $M^2 \gg m_W^2$ and terms actually enhanced by the factor $\Delta M^2/m_W^2$, with ΔM^2 the mass-squared splitting within an isodoublet [8]. The chiral nature of the weak interactions thus increases the power of radiative corrections to illuminate new physics.

In this paper we would like to analyze another set of weak-interaction experiments, to be done at still higher energy. The next step for electron–positron colliders beyond the current generation of Z^0 resonance machines will be to a linear collider with an energy of order 1 TeV in the center of mass. At such a machine, the most important single process contributing to the electron–positron annihilation cross section is the production of W-boson pairs. It is well known that confirmation of the qualitative, tree-level properties of the W-pair production cross section already provides a stringent test of the standard model of weak interactions [9, 10]. The various diagrams contributing to this process, considered individually, grow faster with s than would be permitted by unitarity. The unitarity constraint on the tree-level amplitude is maintained only by virtue of a delicate cancellation among the various diagrams; this cancellation requires the precise gauge-theory form of the vertices coupling W pairs to the photon and the Z^0 [11]. This observation has been used to propose experimental tests of the idea that W bosons are composite states; indeed, models with composite W bosons produce wildly different cross sections from those of the standard model [12].

We observe here that even within the standard model, the introduction of new heavy particles can cause large deviations from the tree-level cross section. New species with perfectly conventional electroweak couplings naturally yield different radiative corrections to the s- and t-channel diagrams involved in the tree-level unitarity cancellation. All of these corrections together must sum to zero (to leading order) for asymptotic s. However, the regime of greatest experimental interest corresponds to the case of a state with mass M too large to allow its pair-production at the high-energy lepton collider: $s \leqslant M^2$, while $s \gg m_W^2$. In this regime, there is no reason for the unitarity cancellations to occur, and, indeed, we find enhanced

radiative corrections of order $(\alpha/\pi)(s/m_W^2)$. These effects can be readily identified experimentally. We call this phenomenon, in which heavy-particle radiative corrections postpone the asymptotic cancellation among diagrams, "unitarity delay".

As a part of our calculation, we will give a simplified analysis of the general structure of radiative corrections to W pair production. The radiative corrections due to the conventional states of the standard model have, of course, been calculated some time ago by Lemoine and Veltman [13], Philippe [14], and others*. However, the structure of the corrections is quite complex, since the theory must be renormalized to the standard model's physical parameters as measured in lower-energy weak interactions. It was observed in ref. [6] that the renormalization program for weak-interaction radiative corrections at the one-loop level is greatly simplified if one assumes that the virtual particles do not couple directly to light leptons but only to the gauge bosons through their standard-model gauge interactions. This assumption is valid for most new particles one might wish to introduce – heavy quarks, heavy leptons, technicolor bosons, and all of the states of supersymmetric theories except the selectron and the smuon. Lynn, Peskin and Stuart termed this scheme of coupling "oblique". They showed that the oblique radiative corrections to the properties of the Z and W can be represented quite generally by straightforward and manifestly finite expressions. These expressions allow one to classify the various corrections and to understand which precision experiments should give identical and which complementary information on new physics. One of our goals in this paper is to extend this analysis to the corrections to $e^+e^- \to W^+W^-$.

Accordingly, this paper will proceed as follows. We begin in sect. 2 by reviewing the basic kinematics of W-pair production. Following the formalism of Hagiwara et al. [18] we present formulae for observable differential cross sections in terms of W-pair form factors, which might then be analyzed at the one-loop level. In sect. 3, we present a general analysis of the oblique weak-interaction radiative corrections to the W form factors. We explicitly extract corrections which are already observable in low-energy and Z^0 resonance experiments, incorporating these into the effective running electroweak parameters defined by Kennedy and Lynn [5]. What remains is a set of intrinsically new radiative effects; we organize these into manifestly ultraviolet-finite combinations. Finally, we evaluate these new corrections for the case of heavy fermions and scalars. In sect. 4 we study the various asymptotic limits of the form factors and confirm the kinematic enhancement of the radiative corrections in the region $s \sim M^2 \gg m_W^2$. We also check explicitly the restoration of the unitarity cancellation for asymptotic s. In sect. 5 we discuss the physics underlying observability of the corrections, and present numerical examples relevant to future high-energy experiments. We find that a new heavy generation of fermions

* See refs. [15, 16, 17]. An extensive bibliography of theoretical work on the reaction $e^+e^- \to W^+W^-$ can be found in ref. [18].

gives a sizeable correction, an enhancement of roughly 0.02 pb, constant in $\cos\theta$. At 1 TeV, this represents a 5% enhancement of the total cross section at non-forward angles.

2. General formalism

Since our analysis concerns oblique corrections due to new heavy particles, we should expect that the most interesting effects we will uncover will be corrections to the form of the three-gauge-boson vertices. It is easiest to keep track of these corrections by studying the reaction $e^+e^- \to W^+W^-$ for vertices of the most general structure, and then inserting the specific expressions for the form factors which arise from explicit one-loop computations. The general analysis which we require has been carried out most efficiently by Hagiwara, Peccei, Zeppenfeld, and Hikasa (HPZH) [18]. In this section, we will review their results and express their formulae in a fashion convenient for our analysis.

HPZH begin their analysis with a general parametrization of the WWA and WWZ vertices. In this paper, we will work in the euclidean metric. With that convention, their general vertex takes the following form: Let f_i^V represent form factors ($V = \mathrm{A}$ or Z) and T_i represent canonical Lorentz structures (implicitly carrying three vector indices). The vertex shown in fig. 1 is built from these ingredients as

$$\begin{aligned}\Gamma_V^{\mu\alpha\beta}(q,\bar{q},P) &\equiv \sum_{i=1}^{7} f_i^V T_i \\ &= f_1^V (q-\bar{q})^\mu \delta^{\alpha\beta} + f_2^V \frac{(q-\bar{q})^\mu P^\alpha P^\beta}{m_W^2} \\ &\quad + f_3^V (P^\alpha \delta^{\mu\beta} - P^\beta \delta^{\mu\alpha}) + f_4^V i (P^\alpha \delta^{\mu\beta} + P^\beta \delta^{\mu\alpha}) \\ &\quad + f_5^V \epsilon^{\mu\alpha\beta\rho} (q-\bar{q})_\rho + f_6^V i \epsilon^{\mu\alpha\beta\rho} P_\rho \\ &\quad + f_7^V i \frac{(q-\bar{q})^\mu \epsilon^{\alpha\beta\rho\sigma} P_\rho (q-\bar{q})_\sigma}{m_W^2} . \end{aligned} \tag{2.1}$$

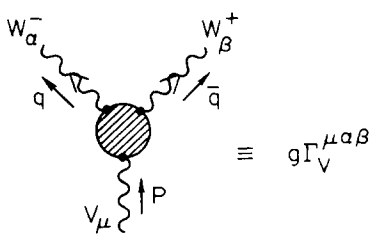

Fig. 1. The general vertex for W pairs.

The form factors are dimensionless functions of s and m_W. We will consistently ignore the electron mass.

At the tree level, the A and Z vertices have the same kinematic structure; both are of the form $g_V T_0$, where

$$g_A = e, \qquad g_Z = e\frac{c_\theta}{s_\theta}, \tag{2.2}$$

(s_θ and c_θ denote $\cos\theta_w$ and $\sin\theta_w$) and

$$T_0 = T_1 + 2T_3 = (q-\bar{q})^\mu \delta^{\alpha\beta} + 2(P^\alpha \delta^{\mu\beta} - P^\beta \delta^{\mu\alpha}). \tag{2.3}$$

Thus, at the tree level, we would write

$$f_1^A = f_1^Z = 1, \qquad f_3^A = f_3^Z = 2, \tag{2.4}$$

and set the other form factors to zero.

Using eq. (2.1), we can write the full amplitude arising from the s-channel diagrams for $e^+e^- \to W^+W^-$ (fig. 2(a)) as

$$\mathcal{M} = ie^2 Q(\bar{v}\gamma_\mu u)\frac{1}{P^2}\Gamma_A^{\mu\alpha\beta}\mathscr{E}_\alpha^*(q)\mathscr{E}_\beta^*(\bar{q})$$

$$+ ie^2\frac{(I_3 - s_\theta^2 Q)}{s_\theta^2}(\bar{v}\gamma_\mu u)\frac{1}{P^2 + m_Z^2}\Gamma_Z^{\mu\alpha\beta}\mathscr{E}_\alpha^*(q)\mathscr{E}_\beta^*(\bar{q}), \tag{2.5}$$

where $P^2 = -s$, u and v are electron and positron Dirac spinors, and $\mathscr{E}_\alpha(q)$, $\mathscr{E}_\beta(\bar{q})$ are polarization vectors of $W^\mp$, respectively. We may consider the electron to have definite helicity and write $I_3 = -\frac{1}{2}$ for e_L, $I_3 = 0$ for e_R. Eq. (2.5) suggests that we

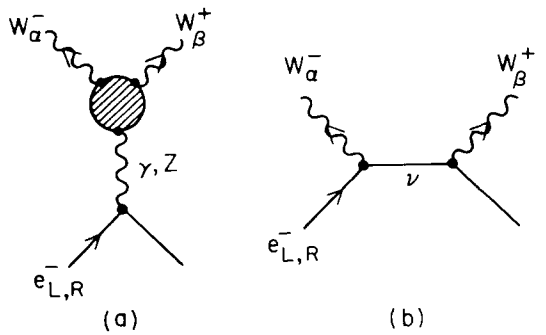

Fig. 2. The amplitude for $e^+e^- \to W^+W^-$: (a) s-channel (general vertex); (b) t-channel.

combine the photon and Z vertices according to

$$F_i = Qf_i^A + \frac{(I_3 - s_\theta^2 Q)}{s_\theta^2}\left(\frac{s}{s - m_Z^2}\right) f_i^Z, \quad i = 1,\ldots,7, \tag{2.6}$$

and define $\Gamma^{\mu\alpha\beta}$ as the vertex built from these form factors according to eq. (2.1)

$$\Gamma^{\mu\alpha\beta}(q,\bar{q},P) = \sum_{i=1}^{7} F_i T_i. \tag{2.7}$$

Then the matrix element (2.5) can be written more concisely as

$$\mathcal{M}_{\pm} = \left(-\frac{ie^2}{s}\right)(\bar{v}\gamma_\mu u)\Gamma^{\mu\alpha\beta}\mathcal{E}_\alpha^*(q)\mathcal{E}_\beta^*(\bar{q}). \tag{2.8}$$

The form factors F_4, F_6, and F_7 multiply *CP*-violating terms; these always vanish explicitly in the standard model and in the *CP*-conserving extensions that we will consider here.

It is quite straightforward to evaluate eq. (2.8) directly for each initial and final polarization state by inserting explicit forms for the electron and positron spinors and the W-boson polarization vectors. We sketch this development in appendix A. Following this analysis, we can construct the differential cross section for W scattering from electron and positron states of definite helicity into W states of definite polarization. Expressing these cross sections in units of the point cross section 1 R $= 4\pi\alpha^2/3s$, we find

$$\frac{d\sigma}{d\cos\theta} = \tfrac{3}{8}\beta \cdot \Sigma\,(\mathrm{R}),$$

$$\Sigma_{TT} = 2\sin^2\theta\left[|A_1|^2 - (A_1A_2^* + A_2A_1^*)\cos\theta + |A_2|^2(1+2\cos^2\theta)\right],$$

$$\Sigma_{TL} = \Sigma_{LT} = |A_3|^2(1+\cos^2\theta) + (A_3A_4^* + A_4A_3^*)\cos\theta\sin^2\theta + |A_4|^2\sin^4\theta,$$

$$\Sigma_{LL} = |A_5|^2\sin^2\theta, \tag{2.9}$$

where θ is the scattering angle in the center-of-mass frame, and the subscripts T, L denote transverse or longitudinal polarization of the W^- and W^+. For $e_R^- + e_L^+$, the *t*-channel diagram does not contribute and so the coefficients A_i are built directly from the F_i

$$A_1 = \beta F_1, \qquad A_2 = 0,$$

$$A_3 = \frac{\beta^2\sqrt{s}}{m_W}\left[\tfrac{1}{2}F_3 + \tfrac{1}{2}\beta\cos\theta F_5\right], \qquad A_4 = \frac{\beta^2\sqrt{s}}{2m_W}F_5,$$

$$A_5 = \beta\frac{s}{m_W^2}\left[\tfrac{1}{2}F_3 - \left(\tfrac{1}{2} - \frac{m_W^2}{s}\right)F_1 + \tfrac{1}{4}\beta^2\frac{s}{m_W^2}F_2\right], \tag{2.10}$$

where β is the W velocity: $\beta = (1 - 4m_W^2/s)^{1/2}$. For $e_L^- + e_R^+$, we find the more complicated result

$$A_1 = \beta F_1 + \frac{\beta}{2s_\theta^2 \mathscr{D}}$$

$$A_2 = \frac{1}{2s_\theta^2 \mathscr{D}}$$

$$A_3 = \frac{\beta\sqrt{s}}{m_W}\left[\tfrac{1}{2}F_3 - \tfrac{1}{2}\beta\cos\theta F_5 + \frac{1}{2s_\theta^2} + \frac{m_W^2}{s_\theta^2\beta^2 s}\left(1 - \frac{2m_W^2}{s\mathscr{D}}\right)\right]$$

$$A_4 = -\frac{\beta^2\sqrt{s}}{2m_W}F_5 + \frac{m_W}{s_\theta^2\sqrt{s}\,\mathscr{D}}$$

$$A_5 = \beta\frac{s}{m_W^2}\left[\tfrac{1}{2}F_3 - \left(\tfrac{1}{2} - \frac{m_W^2}{s}\right)F_1 + \tfrac{1}{4}\beta^2\frac{s}{m_W^2}F_2 + \frac{1}{4s_\theta^2} + \frac{1}{\beta^2 s_\theta^2}\frac{m_W^2}{s}\left(1 - \frac{2m_W^2}{s\mathscr{D}}\right)\right], \tag{2.11}$$

where β is as above and

$$\mathscr{D} = \tfrac{1}{2}(1 + \beta^2 - 2\beta\cos\theta). \tag{2.12}$$

In practice, it is not experimentally straightforward to separate the cross sections for W-pair production into the various polarization states. The easiest way to extract some of the information on the W polarization is to use the decay of the W to a charged lepton. The decay distribution obviously depends on whether the W is longitudinally or transversely polarized. Further, the parity violation in the decay amplitude allows one to distinguish the two transverse polarization states. The explicit formula involves only the form factors A_i of eqs. (2.10) and (2.11). Let χ be the angle between the W momentum vector and the lepton momentum vector as measured in the W rest frame. Then the angular distribution in χ is given by

$$\begin{aligned}\frac{d\sigma}{d\cos\theta\, d\cos\chi}&(e^+e^- \to W^+\ell^-\bar{\nu}) \\ &= \tfrac{9}{32}\beta\,\mathrm{BR}(W^- \to \ell^-\bar{\nu})\big[\Sigma_{TT}(1 - \tfrac{1}{2}\sin^2\chi) \pm 4\cos\theta\sin^2\theta|A_2|^2\cos\chi \\ &\quad + \Sigma_{LT}(1 + \tfrac{1}{2}\sin^2\chi) \pm (2\cos\theta|A_3|^2 + \sin^2\theta(A_3A_4^* + A_4A_3^*))\cos\chi \\ &\quad + \Sigma_{LL}\sin^2\chi\big],\end{aligned} \tag{2.13}$$

where the upper (lower) sign refers to the cross section for $e_L^- e_R^+$ ($e_R^- e_L^+$). The same formula holds for the χ distributions in $e^+e^- \to W^-\ell^+\nu$ from each electron polarization state. This formula agrees with HPZH; it is a simple byproduct of the analysis leading to eq. (2.9). We discuss its derivation in appendix A.

The tree-level differential cross sections predicted by eqs. (2.9) and (2.13) are shown in fig. 3. In fig. 3a, we display the differential cross section predicted for W-pair production by unpolarized e^+e^- pairs at $\sqrt{s} = 1$ TeV and the decomposition of the cross section into the contributions from the various W-boson polarization states. (In principle, one might also consider the effect of polarizing the electrons; however, the contribution from right-handed electrons is generally quite small.) In fig. 3b, we plot the χ distribution at three values of $\cos\theta$. The change in the form of this distribution reflects the increasing proportion of longitudinally polarized W bosons produced as one moves toward the backward direction.

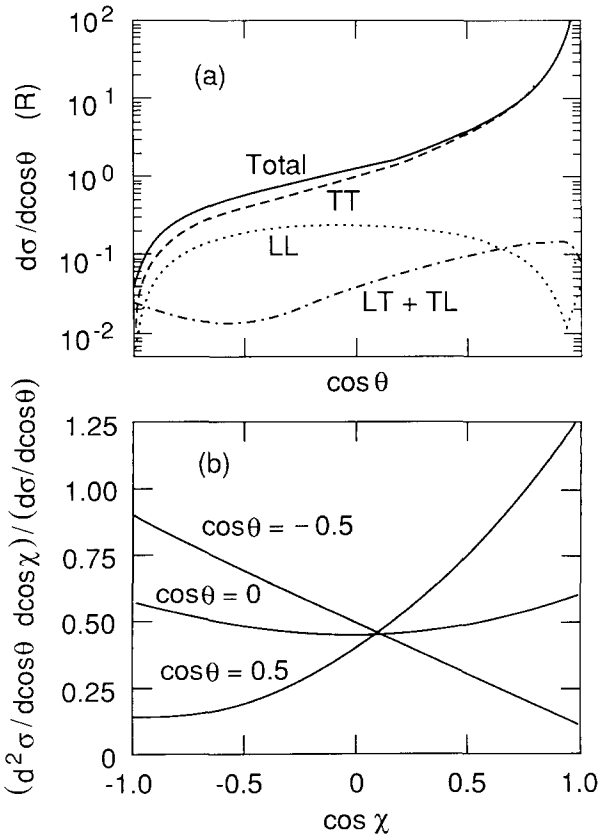

Fig. 3. (a) Tree-level differential cross section versus θ: longitudinal polarizations only (LL), mixed polarizations (LT), transverse polarizations (TT), and their sum. (b) Tree-level χ-distribution ratio.

Since the A_i are dimensionless scattering amplitudes, they will violate the unitarity limit if they grow asymptotically with any positive power of s. For example, eqs. (2.10) and (2.11) show clearly that A_5 will violate unitarity if the combination of form factors in brackets has asymptotic s^0 behavior, since this amplitude contains an overall factor s/m_W^2 arising from the scalar product of longitudinal polarization vectors. At the tree level, eqs. (2.4) and (2.6) give

$$F_1 = \tfrac{1}{2}F_3 = \frac{I_3}{s_\theta^2}\left(1 + \frac{m_Z^2}{s}\right) + \frac{m_Z^2}{s} + \ldots . \tag{2.14}$$

Examining eqs. (2.10) and (2.11) we see that for right-handed electrons, $I_3 = 0$ and the unitarity cancellation is immediate. For left-handed electrons, with $I_3 = -\frac{1}{2}$, the residual term from the form factors is cancelled by the constant term $1/4s_\theta^2$, which represents the asymptotic behavior of the t-channel diagram.

This type of cancellation should occur order-by-order in perturbation theory. In sect. 4, we will show this explicitly for one-loop radiative corrections due to a heavy generation. The cancellation guarantees good asymptotic behavior up to logarithmic factors. However, the cancellation is guaranteed only for values of s which are actually asymptotic. A new heavy particle of mass M could potentially produce very large radiative corrections by disturbing the delicate cancellations in A_5 at energies of order M if $M \gg m_W$. In sect. 3, we will explain how to compute the corrections to the form factors F_i which allow us to analyze that situation.

3. One-loop radiative corrections

It will be useful to consider the various contributions systematically before beginning an explicit computation of the one-loop corrections. In this paper we deal only with oblique corrections; this still includes a variety of corrections, as we show in fig. 4. In the standard model, as long as we have no subdiagrams which involve Higgs–Higgs or W–W scattering processes (as is the case here), the divergences of all one-loop diagrams are removed when we adjust three basic parameters, which may be taken to be g, g' and the Higgs vacuum expectation value or, more concretely, α, G_μ, and m_Z. In this section, we will explain how to renormalize the various diagrams of fig. 4 and organize them into finite corrections with direct physical meaning.

We would particularly like to address the question of which part of the one-loop corrections to $e^+e^- \to W^+W^-$ are already constrained by measurements at low energy or at the Z^0 and which are new to the W-pair production process. To make this separation, we follow Kennedy and Lynn [5] in parameterizing our amplitudes in terms of running electroweak parameters; ref. [5] shows in detail how these quantities summarize the information on weak-interaction radiative corrections

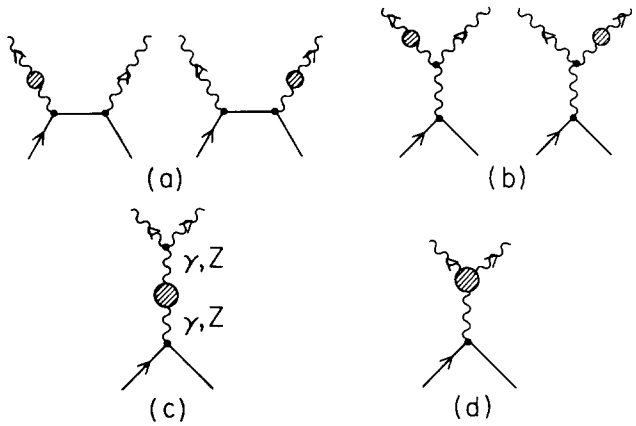

Fig. 4. One-loop oblique corrections to $e^+e^- \to W^+W^-$: (a) corrections to the t-channel diagram; (b) external leg corrections to the s-channel diagram; (c) propagator corrections to the s-channel diagram; (d) vertex corrections to the s-channel diagram.

available from low-energy experiments. From the remaining corrections, we will also extract a finite overall factor representing the W-boson wave-function renormalization. This will leave over other finite contributions which correct the various form factors f_i^V in the three-gauge-boson vertices. These are the corrections which have the largest physical effect on W-pair production.

We begin our analysis by presenting our notation for the loop corrections. These will be given at first in terms of bare parameters (which always carry a subscript 0). The boson self-energies will be denoted $\Pi_{VV'}(P^2)$, as in fig. 5. We define

$$\Pi^p_{VV'} \equiv \frac{\Pi_{VV'}}{P^2}\,.$$

The various boson self-energies can be written as two-point functions of the electromagnetic currents j^μ_{EM} and the weak isospin currents $j^{\mu i}_{\mathrm{L}}$ according to

$$\Pi_{\mathrm{AA}} = e_0^2 \Pi_{QQ}\,,$$

$$\Pi_{\mathrm{ZA}} = \frac{e_0^2}{s_0 c_0}\left(\Pi_{3Q} - s_0^2 \Pi_{QQ}\right),$$

$$\Pi_{\mathrm{ZZ}} = \frac{e_0^2}{s_0^2 c_0^2}\left(\Pi_{33} - 2 s_0^2 \Pi_{3Q} + s_0^4 \Pi_{QQ}\right),$$

$$\Pi_{\mathrm{WW}} = \frac{e_0^2}{s_0^2}\Pi_{11}\,, \tag{3.1}$$

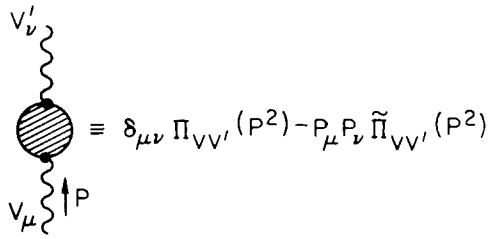

Fig. 5. Notation for vector-boson self-energies.

where $s_0 = \sin\theta_0$ and $c_0 = \cos\theta_0$ are defined by $s_0 = e_0/g_0$. In general, only the real parts of these amplitudes are relevant to the $O(\alpha)$ corrections.

Following ref. [5], we can use Dyson's equations to account for vacuum polarization and boson self-energies by exchanging the bare coupling constants for renormalized, running coupling constants (subscripted with a star). This results in an effective lagrangian with the same form as $\mathscr{L}_0$, but with all bare quantities replaced by asterisked quantities. To include the effects of the oblique corrections we are accounting here, we thus write

$$\begin{aligned}
\frac{1}{e_*^2(P^2)} &= \frac{1}{e_0^2} - \Pi_{QQ}^{p}(P^2) \\
&= \frac{1}{e_*^2(\mu^2)} - \left[\Pi_{QQ}^{p}(P^2) - \Pi_{QQ}^{p}(\mu^2)\right], \\
\frac{1}{g_*^2(P^2)} &= \frac{1}{g_0^2} - \Pi_{3Q}^{p}(P^2) \\
&= \frac{1}{g_*^2(\mu^2)} - \left[\Pi_{3Q}^{p}(P^2) - \Pi_{3Q}^{p}(\mu^2)\right];
\end{aligned} \tag{3.2}$$

from these we define $s_*^2 = e_*^2/g_*^2$ and $c_*^2 = 1 - s_*^2$. These formulae allow us to relate processes occurring at P^2 to measurements performed at μ^2. We similarly define running boson mass parameters to include self-energy and mixing effects

$$M_{Z_*}^2 = \frac{e_*^2}{s_*^2 c_*^2}\frac{1}{4\sqrt{2}\,G_{\mu_*}\rho_*}, \qquad M_{W_*}^2 = \frac{e_*^2}{s_*^2}\frac{1}{4\sqrt{2}\,G_{\mu_*}}, \tag{3.3}$$

with

$$G_{\mu_*}(P^2) = \frac{G_{\mu_*}(\mu^2)}{1 - 4\sqrt{2}\, G_{\mu_*}(\mu^2)(\Pi_{11} - \Pi_{3Q})|_{\mu^2}^{P^2}} \tag{3.4}$$

$$\rho_*(P^2) = \frac{1}{1 - 4\sqrt{2}\, G_{\mu_*}(\Pi_{33} - \Pi_{11})}\,. \tag{3.5}$$

(All starred quantities in this paper should be evaluated at P^2, unless explicitly written otherwise.) A little algebra yields an explicit form

$$\begin{aligned} M_{Z_*}^2(P^2) = m_Z^2 + \frac{g_*^2}{c_*^2}\Big[&(\Pi_{3Q} - \Pi_{33})(P^2) - (\Pi_{3Q} - \Pi_{33})(-m_Z^2) \\ &+ m_Z^2(c_*^2 - s_*^2)\big(\Pi_{3Q}^p(P^2) - \Pi_{3Q}^p(-m_Z^2)\big) \\ &+ m_Z^2 s_*^4\big(\Pi_{QQ}^p(P^2) - \Pi_{QQ}^p(-m_Z^2)\big)\Big]\,. \end{aligned} \tag{3.6}$$

The combination of self-energies on the right-hand side of eq. (3.6) has no uncancelled ultraviolet divergences. With these definitions and light external fermions, the boson propagator and non-abelian vertex contributions to the neutral-current interactions sum to the fully renormalized expression [5]

$$\mathcal{M} = \left\{ e_*^2 \frac{QQ'}{-s} + \frac{e_*^2}{s_*^2 c_*^2} \frac{(I_3 - s_*^2 Q)(I_3' - s_*^2 Q')}{-s + M_{Z_*}^2} \right\}. \tag{3.7}$$

We use the renormalization scheme detailed in ref. [5]

$$\begin{aligned} m_Z^2 &\equiv M_{Z_*}^2\big(P^2 = -m_Z^2\big) = (93.00\ \text{GeV})^2\,, \\ 4\pi/e_*^2(0) &= 137.036\,, \\ G_{\mu_*}(0) &= 1.1581 \times 10^{-5}\ (\text{GeV})^{-2}\,. \end{aligned} \tag{3.8}$$

(G_μ differs from $G_{\mu_*}(0)$ by residual vertex and box corrections.) All of the divergences in our calculation will be absorbed into the three functions $M_{Z_*}^2$, e_*^2, and g_*^2 or s_*^2. Note that in this renormalization scheme, $s_*^2(-m_Z^2)$ is extracted from the measured m_Z through terms including ρ_*. Thus, $s_*^2(-m_Z^2)$ will be affected by large isospin mass splittings.

With this renormalization, contributions from individual fermion generations or scalar doublets are separately gauge invariant and finite; each such contribution can

be considered on its own footing. Accordingly, while our calculations include all electroweak effects of the new heavy particles, they ignore the conventional particles of the standard model, since the standard effects are of order α, unenhanced, and smooth as a function of s. The standard contributions should of course be included to correctly analyze precision measurements. We also neglect minor corrections from the Higgs and vector-boson sector; this eliminates longitudinal self-energy contributions and the need to rediagonalize the Z and photon [5]. (The case of a strongly coupled Higgs sector will be presented in a separate publication [19].) Bremsstrahlung effects merely produce an overall multiplicative factor convolved with a hard-photon energy shift, which can be treated [20] straightforwardly and will have no qualitative influence on the effects reported here. Finally, QCD corrections should be quite small at the energies we consider, and we neglect them as well.

In our formulae, the influence of the running of e_*^2 and s_*^2 is relatively minor, and the reader may reproduce the value of any differential cross section that we present to a few percent accuracy by fixing these running parameters at the values

$$4\pi/e^2 = 128.0, \qquad s_\theta^2 = 0.223; \tag{3.9}$$

s_θ^2 will be affected by the ρ parameter of course. The W-boson mass, unlike the Z mass, appears in our calculation only from the kinematics and should be set directly at its physical value. In the calculations of sect. 5, we have used the value of $m_W^2 \equiv M_{W_*}^2(-m_W^2)$ computed from the electroweak theory, including one-loop radiative corrections. This means that we change m_W slightly in accord with the properties of the new heavy particles; this change is small except when we include heavy generations with very large isospin splitting. Even in the worst case which is consistent with current ρ parameter measurements ($|\rho - 1| < 1\%$, translating to $\Delta m^2 < (200\ \text{GeV})^2$) [21,22], one would make an error of less than 2% in the differential cross section by taking the value $m_W = 82$ GeV.

Having defined the parameters of the theory, we can now put together the various corrections to $e^+e^- \to W^+W^-$. We begin with the external leg corrections shown in figs. 4a and b. These multiply the matrix element by an overall wave-function-renormalization factor

$$Z_W = 1 + g_0^2 \left(\frac{\partial}{\partial P^2} \Pi_{11} \right) \Bigg|_{P^2 = -m_W^2}. \tag{3.10}$$

For the t-channel diagram, this is the only one-loop correction. If we recall that the bare tree diagram is proportional to g_0^2, we can rewrite the overall factor so as to have the same g_*^2 appearing in both channels

$$g_0^2 Z_W = g_*^2(P^2) \frac{g_0^2}{g_*^2} Z_W = g_*^2(P^2)\xi, \tag{3.11}$$

where

$$\xi \doteq 1 + g_*^2(P^2)\left(\Pi'_{11}(-m_W^2) - \Pi^p_{3Q}(P^2)\right). \tag{3.12}$$

Since a Ward identity relates vertex and leg corrections, this is a finite object, as may be checked explicitly.

The easiest way to analyze the s-channel diagrams is to use the effective-lagrangian insight in eq. (3.7) that the diagrams of the form of fig. 4c simply renormalize the parameters of the zeroth-order diagrams. Folding these corrections into the zeroth-order amplitude, we have

$$\mathcal{M} = \left(-\frac{ie_*^2}{s}\right)(\bar{v}\gamma_\mu u)\left[Q + \frac{(I_3 - s_*^2 Q)}{s_*^2}\frac{s}{s - M_{Z_*}^2}\right](T_0)^{\mu\alpha\beta}\mathcal{E}_\alpha^*(q)\mathcal{E}_\beta^*(\bar{q}), \tag{3.13}$$

where T_0 is the tensor (2.3). We then consider the diagrams of fig. 4b to multiply this amplitude by the additional and divergent factor

$$Z_W = \xi\left(1 + g_*^2 \Pi^p_{3Q}(P^2)\right). \tag{3.14}$$

Finally, we must include the true vertex corrections shown in fig. 4d. In order to keep track of the electroweak currents as in eq. (3.1), we notate these corrections as

$$\Gamma_A^{\mu\alpha\beta} \equiv e_* g_*^2 \Sigma_{Q+-}^{\mu\alpha\beta}, \qquad \Gamma_Z^{\mu\alpha\beta} \equiv \frac{e_*}{s_* c_*} g_*^2 \left(\Sigma_{3+-}^{\mu\alpha\beta} - s_*^2 \Sigma_{Q+-}^{\mu\alpha\beta}\right), \tag{3.15}$$

using $g_0^2 = g_*^2$ to the required accuracy. Then the diagrams of fig. 4d yield an additional term

$$\mathcal{M} = \left(-\frac{ie_*^2}{s}\right)(\bar{v}\gamma_\mu u)$$
$$\times\left[Q\Sigma_{Q+-}^{\mu\alpha\beta} + \frac{(I_3 - s_*^2 Q)}{s_*^2 c_*^2}\frac{s}{(s - m_Z^2)}\left(\Sigma_{3+-}^{\mu\alpha\beta} - s_*^2 \Sigma_{Q+-}^{\mu\alpha\beta}\right)\right]\mathcal{E}_\alpha^*(q)\mathcal{E}_\beta^*(\bar{q}). \tag{3.16}$$

Here we can neglect the $O(g^2)$ difference between $M_{Z_*}^2$ and m_Z^2, although in eq. (3.13) we must retain corrections proportional to $M_{Z_*}^2 - m_Z^2$. There it is useful to expand the denominator $(s - M_{Z_*}^2)$ to first order about $(s - m_Z^2)$; then the zeroth-order term can enter the tree-level unitarity cancellation unchanged. The results of eqs. (3.13), (3.14) and (3.16) can thus be combined to form the following expression

for the sum of the s-channel diagrams

$$\mathcal{M} = \left(-\frac{ie_*^2}{s}\right)\xi(\bar{v}\gamma_\mu u)\left\{\left[Q + \frac{(I_3 - s_*^2 Q)}{s_*^2}\frac{s}{s - m_Z^2}\right]\cdot T_0^{\mu\alpha\beta}\right.$$

$$+ \frac{(I_3 - s_*^2 Q)}{s_*^2}\frac{s}{s - m_Z^2}\frac{M_{Z_*}^2 - m_Z^2}{s - m_Z^2}T_0^{\mu\alpha\beta}$$

$$+ \left[Q\cdot g_*^2\left(\Sigma_{Q+-}^{\mu\alpha\beta} + \Pi_{3Q}^p T_0^{\mu\alpha\beta}\right) + \frac{(I_3 - s_*^2 Q)}{s_*^2 c_*^2}\frac{s}{s - m_Z^2}\right.$$

$$\left.\left.\times g_*^2\left(\Sigma_{3+-}^{\mu\alpha\beta} - s_*^2\Sigma_{Q+-}^{\mu\alpha\beta} + c_*^2\Pi_{3Q}^p T_0^{\mu\alpha\beta}\right)\right]\right\}$$

$$\times\mathscr{E}_\alpha^*(q)\mathscr{E}_\beta^*(\bar{q}). \tag{3.17}$$

Each line of eq. (3.17) has cancelling ultraviolet divergences, since Σ_{Q+-}, Σ_{3+-}, and $-\Pi_{3Q}^p T_0$ contain identical divergences. In the first line, we have separated out a piece proportional to the zeroth order s-channel amplitude; when this is added to the t-channel amplitude, the sum is simply the zeroth-order amplitude evaluated with running coupling constants and multiplied by ξ. The remaining three lines of eq. (3.17) give intrinsically new corrections.

We expect that the full one-loop-corrected amplitude should obey perturbative unitarity. In the combination of the t-channel amplitude with the first line of eq. (3.17), the unitarity cancellation is explicit; eq. (3.11) arranges for both channels to have $g_*^2(P^2)$ as the coupling and ξ as an overall factor. For the remaining terms in eq. (3.17), we can only check case-by-case that the leading, unitarity-violating s dependence cancels when s is large. If the loop diagrams contain a heavy species of mass M, we cannot expect this cancellation to occur except when $s \gg M^2$. Thus, when $s \sim M^2 \gg m_W^2$, we expect the last three lines of eq. (3.17) to produce radiative corrections enhanced by a factor (s/m_W^2). These are the dominant effects arising from our analysis.

We conclude this section by converting the amplitude (3.17) into a set of form factors which can be inserted into the formulae of sect. 2. If we use $T_0 = T_1 + 2T_3$ and decompose each vertex function according to

$$\Sigma^{\mu\alpha\beta} \equiv \sum_{i=1}^{7} T_i \Sigma^{(i)}, \tag{3.18}$$

we can read from eq. (3.17)

$$f_1^A = 1 + g_*^2\left[\Sigma_Q^{(1)} + \Pi_{3Q}^p\right],$$

$$f_1^Z = 1 + \frac{g_*^2}{c_*^2}\left[\left(\Sigma_3^{(1)} - s_*^2\Sigma_Q^{(1)}\right) + c_*^2\Pi_{3Q}^p\right] + \frac{M_{Z_*}^2 - m_Z^2}{s - m_Z^2},$$

$$f_3^A = 2 + g_*^2\left[\Sigma_Q^{(3)} + 2\Pi_{3Q}^p\right],$$

$$f_3^Z = 2 + \frac{g_*^2}{c_*^2}\left[\left(\Sigma_3^{(3)} - s_*^2\Sigma_Q^{(3)}\right) + 2c_*^2\Pi_{3Q}^p\right] + 2\frac{M_{Z_*}^2 - m_Z^2}{s - m_Z^2},$$

$$f_i^A = g_*^2\left[\Sigma_Q^{(i)}\right],$$

$$f_i^Z = \frac{g_*^2}{c_*^2}\left[\left(\Sigma_3^{(i)} - s_*^2\Sigma_Q^{(i)}\right)\right], \qquad i = 2,5. \tag{3.19}$$

To use these form factors, we must also make two modifications in the formulae of sect. 2. First, the coupling constants e^2, s_θ^2 should be replaced by e_*^2, s_*^2; second, the final cross sections should be multiplied by the factor $|\xi|^2$ defined in eq. (3.12). Both of these corrections are numerically quite small, although one should note that, for light fermions or scalars, ξ contains logarithmic factors which are important in the correct coupling-constant evolution of the three-gauge-boson vertex.

4. Low- and high-energy behavior

We are now in a position to evaluate the various Feynman diagrams contributing one-loop corrections to the process $e^+e^- \to W^+W^-$ and to organize the results explicitly into finite corrections. For heavy fermions, we consider the diagrams shown in figs. 6a, b. The actual formulae for the various corrections are complicated and, in themselves, rather unilluminating, so we have chosen to display these expressions only in appendix B. In this section and the next, we will discuss their important properties. Here, we analyze the formulae analytically in the limits of high and low energy. For a heavy generation of mass M we will show explicitly the presence of enhanced radiative corrections when $s \ll M^2$ and also a perturbative unitarity cancellation in the radiative corrections for $s \gg M^2$. In sect. 5 we will study the formulae numerically for general values of s.

In our presentation of the complete results given in appendix B, we have followed the method of Passarino and Veltman [23] in expressing the various diagrams in terms of a fixed set of standard one-loop integrals. One can then evaluate these integrals analytically [24]; tailored computer programs exist for this purpose [25, 26]. In our analysis, we have found it convenient to make some further simplifications,

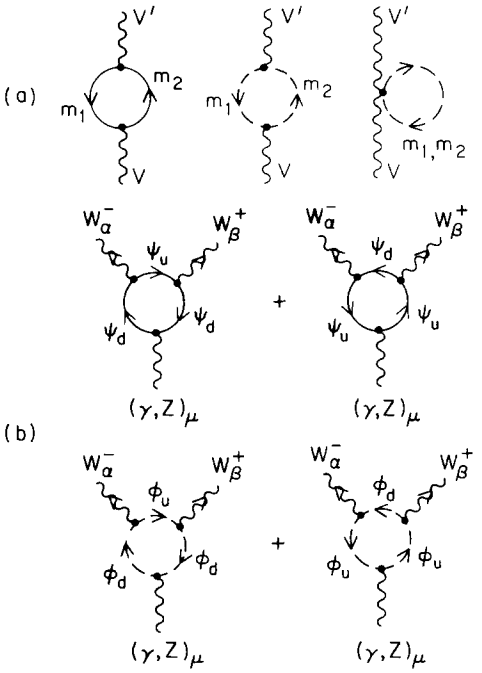

Fig. 6. Feynman diagrams renormalizing the amplitude for $e^+e^- \to W^+W^-$: (a) two-point functions; (b) three-point functions.

including the explicit cancellation of ultraviolet divergences, and to write our results in terms of a set of finite and dimensionless reduced Passarino–Veltman functions. These functions are defined, and their asymptotic forms are presented, in appendix C. The results of this section can then be obtained by inserting the appropriate asymptotic formulae into the results for the form factors given in appendix B.

4.1. NONDECOUPLING EFFECTS AT LOW ENERGY

We consider first the case of radiative corrections for s well below the heavy fermion threshold. As we have explained, we expect in this region to find terms enhanced by a factor (s/m_W^2). Ordinarily, one might expect that loop corrections due to heavy fermions are suppressed by powers of (s/M^2) because of Appelquist–Carazzone decoupling. However, with chiral currents or large doublet mass splittings, it is possible to evade the decoupling theorem and isolate a finite contribution. Clearly, degenerate scalar particles will not exhibit this effect, as we discuss in sect. 5.

Let us then expand the expressions of appendix B, for s in the range $m_W^2 \ll s \ll M^2$, assuming a fermion doublet with hypercharge Y and masses m_u and m_d. Defining

$$\Delta m^2 = m_u^2 - m_d^2 \quad \text{and} \quad m^2 = \tfrac{1}{2}\left(m_u^2 + m_d^2\right), \tag{4.1}$$

with $\Delta m^2 \ll m^2$, we find

$$F_1 \cong \frac{\alpha}{4\pi s_\theta^2}\left[-Y\frac{1}{3c_\theta^2}\frac{\Delta m^2}{m^2} + \frac{I_3}{s_\theta^2 c_\theta^2}\left(-\tfrac{1}{6}c_\theta^2 - Y\tfrac{1}{3}s_\theta^2\frac{\Delta m^2}{m^2}\right)\right],$$

$$F_2 \cong 0,$$

$$F_3 \cong \frac{\alpha}{4\pi s_\theta^2}\left[-Y\frac{7}{12c_\theta^2}\frac{\Delta m^2}{m^2} + \frac{I_3}{s_\theta^2 c_\theta^2}\left(-\frac{c_\theta^2}{3} - Y\frac{7s_\theta^2}{12}\frac{\Delta m^2}{m^2}\right)\right],$$

$$F_5 \cong \frac{\alpha}{4\pi s_\theta^2}\left[-\frac{1}{24c_\theta^2}\frac{\Delta m^2}{m^2} - Y\tfrac{1}{3}\left(1+\frac{1}{c_\theta^2}\right) + \frac{I_3}{s_\theta^2 c_\theta^2}\left(-\tfrac{1}{3}Y - \frac{1}{24}\frac{\Delta m^2}{m^2}\right)\right], \quad (4.2)$$

where $I_3 = -\frac{1}{2}, 0$ for e_L^-, e_R^-. These formulae simplify dramatically if we include a full generation in which all the doublets have the same masses, namely, $[\Delta m^2/m^2]_{\text{lepton}} = [\Delta m^2/m^2]_{\text{quark}}$, and use the fact $\Sigma_{\text{doublets}}\, Y = 0$;

$$F_1 \cong \frac{\alpha}{4\pi s_\theta^2}\left(-\frac{2I_3}{3s_\theta^2}\right), \qquad F_2 \cong 0,$$

$$F_3 \cong \frac{\alpha}{4\pi s_\theta^2}\left(-\frac{4I_3}{3s_\theta^2}\right),$$

$$F_5 \cong \frac{\alpha}{4\pi s_\theta^2}\left(\frac{I_3}{s_\theta^2}+1\right)\left(-\frac{1}{6c_\theta^2}\frac{\Delta m^2}{m^2}\right). \quad (4.3)$$

Note that only F_5 depends on the mass splitting and F_1, F_2 and F_3 are zero for the right-handed electron. For left-handed electrons, the process $e^+e_L^- \to W_L^+W_L^-$ will show leading behavior

$$A_5(1-\text{loop}) \cong \frac{s}{m_W^2}\frac{\alpha}{4\pi s_\theta^2}\frac{1}{6s_\theta^2}, \quad (4.4)$$

and the cross section for $e^+e_L^- \to W_L^+W_L^-$ becomes

$$\frac{d\sigma}{d\Omega} \cong \frac{d\sigma}{d\Omega}(\text{tree})\left[1 + 2\frac{A_5(1-\text{loop})}{A_5(\text{tree})}\right], \quad (4.5)$$

where A_5(tree) is given by eq. (2.11); thus

$$\frac{\delta(d\sigma/d\Omega)}{(d\sigma/d\Omega)} \cong \left(\frac{\alpha c_\theta^2}{3\pi s_\theta^2}\right)\frac{s}{m_W^2} \cong (2.9\times 10^{-3})\frac{s}{m_W^2}. \tag{4.6}$$

This radiative correction is proportional to the number of heavy generations; aside from the effects of isospin mass splittings on the ρ parameter, it does not depend on the masses of the heavy generation as long as $s \ll m^2$ and lepton/quark mass differences are small. The factor 10^{-3} is typical of one-loop radiative corrections, but the enhancement factor s/m_W^2 yields a 10% effect for $\sqrt{s} = 500$ GeV. This relative enhancement continues rising, quadratically in energy, until it is cut off above threshold. In essence, the unitarity delay effect can be thought of as adding a constant 0.02 pbarn to a tree-level cross section which is falling like $1/s$. The unitarity delay thus exists and is measurable at lower energies, but it would be advantageous to use as high an energy as possible.

4.2. ASYMPTOTIC BEHAVIOR AT HIGH ENERGY

We now consider the case $s \gg m^2 \gg m_W^2$, including one heavy generation where all fermions are of equal mass m. As already mentioned in sect. 2, any uncancelled leading s^0 behavior in the form factors F_i will violate unitarity because of the factor s/m_W^2 in A_5. We check this cancellation below, keeping next-to-leading order terms as a check on our numerical results and to provide physical insight into the system's high-energy behavior.

Referring to the appendices, the F_i can be seen to tend asymptotically to

$$\begin{aligned}
F_1 &\cong -\frac{\alpha}{4\pi s_\theta^2}\frac{2}{3}\frac{I_3}{s_\theta^2},\\
\frac{s}{m_W^2}F_2 &\cong -\frac{\alpha}{4\pi s_\theta^2}\left[\frac{4}{3}\frac{I_3}{s_\theta^2} + \frac{m^2}{s}\frac{I_3}{s_\theta^2}\left(32 - 16\ln\frac{s}{m^2} + 4\ln^2\frac{s}{m^2} - 4\pi^2\right)\right],\\
F_3 &\cong -\frac{\alpha}{4\pi s_\theta^2}\frac{m^2}{s}\left[\frac{4}{c_\theta^2}\left(1 + \frac{I_3}{s_\theta^2}\right)\left[\ln\frac{s}{m^2} - 2\right] - 2\frac{I_3}{s_\theta^2}\left[\ln^2\frac{s}{m^2} - \pi^2\right]\right],\\
F_5 &\cong 0;
\end{aligned} \tag{4.7}$$

thus

$$A_5(1\text{-loop}) \cong -\frac{\alpha}{4\pi s_\theta^2}\frac{m^2}{m_W^2}\left(\frac{I_3}{s_\theta^2}\left(\frac{2}{c_\theta^2} - 4\right) + \frac{2}{c_\theta^2}\right)\left[\ln\frac{s}{m^2} - 2\right]. \tag{4.8}$$

Notice that the leading s^0 terms in the F_i are cancelled in A_5, a result of unitarity cancellation at the one-loop level. Also cancelled are all dilogarithms. Even so, if $m^2 \gg m_W^2$ then the magnitude of A_5(1-loop) can be as large as that of A_5(tree) in eqs. (2.10) and (2.11). The perturbative expansion requires careful examination at high energy with a sufficiently heavy fermion generation, as we shall discuss in detail in sect. 5.

5. Numerical results and discussion

We can now compare the above results with numerical calculations and discuss the experimental observability of the heavy-particle corrections. In assessing the size of these corrections, one should remember that nondecoupling effects generally arise from the breaking of global symmetries in association with large dimensionless parameters. For heavy fermions in the standard model, these parameters might arise either from isospin-breaking mass differences or from the large Yukawa couplings needed to generate even large isospin-symmetric masses. We should assess the relative importance of these two contributions. For scalars, only the isospin splitting of masses arises from a symmetry breaking, and so here there is only one possible source for the effect.

Let us begin with the case of heavy, isospin-degenerate fermions. The detailed forms of the radiative corrections to the W form factors, valid over the full range of energies, are presented in appendix B. By inserting these expressions into eq. (2.9), we obtain the effects of the heavy fermions on the differential cross section for W-pair production. In fig. 7, we plot the corrected differential cross section at $\cos\theta = 0$, incorporating effects of a degenerate heavy generation of fermions, for several different masses. (Integration over $\cos\theta$ merely shifts the whole curve upward by including the unenhanced forward peak). We can see that the radiative correction gives a small but noticeable effect at low energies and contributes a significant enhancement of the cross section in a region within a factor of 2 in $\sqrt{s}$ of the pair-production threshold. The suggestion from the analytic formulae of an effect increasing quadratically with energy is actually well confirmed by the numerical results shown in fig. 7. Note the rapid onset of unitarity cancellations above threshold.

The physics of the correction terms is clarified by a more detailed look at the numerical results. Since the delayed unitarity cancellation affects mainly the cross section for producing pairs of longitudinal W bosons, we should expect that the enhanced radiative corrections appear mainly in that polarization state. Indeed, fig. 8 shows the contributions to the cross sections of fig. 7 from longitudinally polarized W pairs; the enhancement of this polarization state is very large and accounts for essentially the whole effect. The heavy fermions make at most a 2% correction to the cross section due to the other polarization states. The importance of the longitudinal W pairs can be assessed in another way, which can be observed

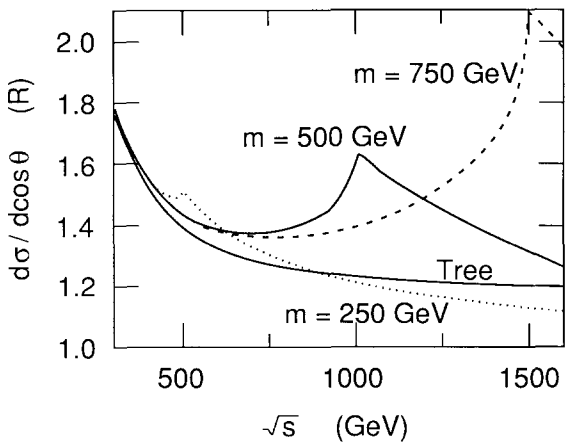

Fig. 7. Corrections to the differential cross section for $e^+e^- \to W^+W^-$ with various degenerate fermion masses, at $\cos\theta = 0$.

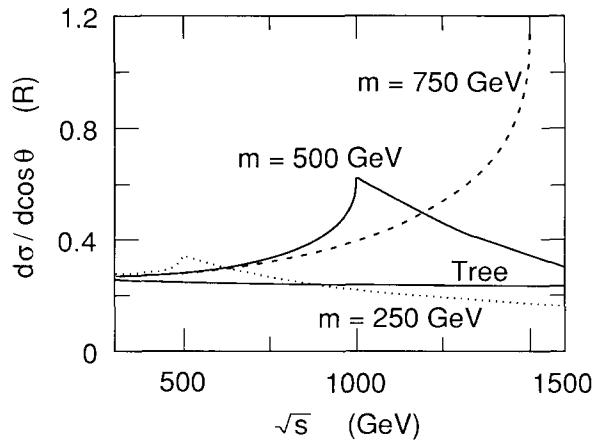

Fig. 8. Contribution to fig. 7 from longitudinal polarizations only, at $\cos\theta = 0$.

directly in experiments: in fig. 9, we plot the distribution of the lepton decay angle $\cos\chi$ in the presence of heavy fermion corrections. The enhancement near $\cos\chi = 0$ indicates the increasing importance of longitudinally polarized W bosons. The dependence on $\cos\theta$ of the heavy fermion corrections shows less structure; the corrections are roughly independent of $\cos\theta$. However, for $\cos\theta > 0.5$, the W-pair production cross section is dominated by transversely polarized pairs, and the relative enhancement due to radiative corrections disappears.

Eq. (4.6) displays the low-energy limit of the correction term. Well below threshold, this contribution is independent of the heavy fermion masses. We

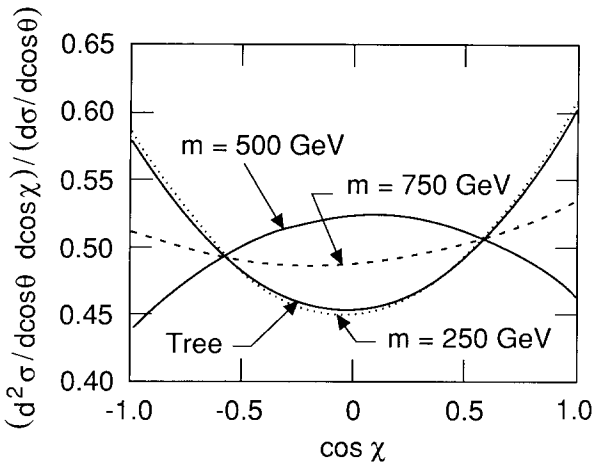

Fig. 9. Corrections to the χ distributions at $\cos\theta = 0$, for degenerate fermions.

confirm this result in fig. 10 by plotting the differential cross section at $\cos\theta = 0$ for relatively low energies. The 3% shift indicated in the figure is just that predicted by eq. (4.6), diluted by the inclusion of the other W polarization states.

Introducing an isospin-breaking mass splitting for the fermion or doublets breaks the standard model's custodial SU(2) symmetry. This is known to lead to a large renormalization of the ρ parameter. In W-pair production, however, such a mass splitting does not generate additional large contributions; rather, its main effect is simply to split the existing peak of the correction term into two. Fig. 11 illustrates

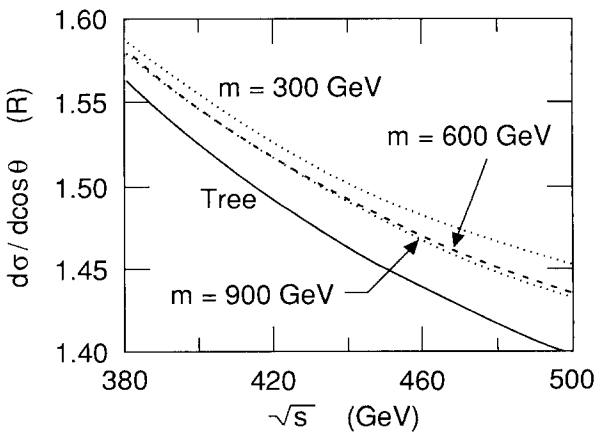

Fig. 10. Corrections to the differential cross section at $\cos\theta = 0$ at low energies, showing the approximate mass independence of the fermion corrections. The 300 GeV fermions are approaching threshold.

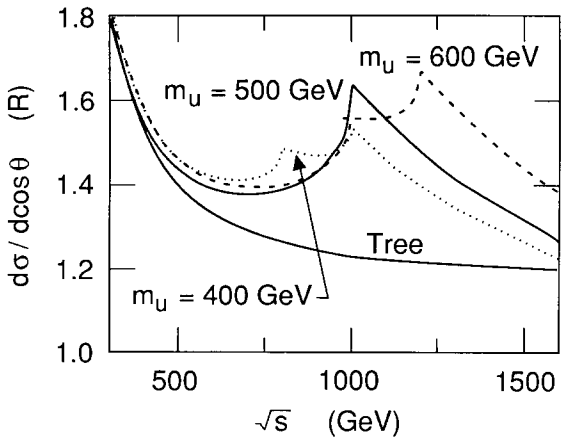

Fig. 11. Peak structure for split fermion doublets; $m_d = 500$ GeV, $\cos\theta = 0$.

this behavior in the differential cross section at $\cos\theta = 0$, for $m_u - m_d = \pm 100$ GeV. The vertex corrections do give a small additional effect proportional to the mass splitting, visible in the last line of eq. (4.3). However, this term contributes only to Σ_{LT} of eq. (2.9), and so it is unimportant at high energies. The pattern of shifts at low energy shown in fig. 12 comes simply from the shifts of m_W and $s_*^2(-m_Z^2)$ due to the renormalization of the ρ parameter; we note again that present data limit isospin mass splittings to $\Delta m^2 < (200\ \text{GeV})^2$ [22].

Since the corrections to the tree-level cross sections we have found are so large, we must address the question of their reliability. On the one hand, we have seen that

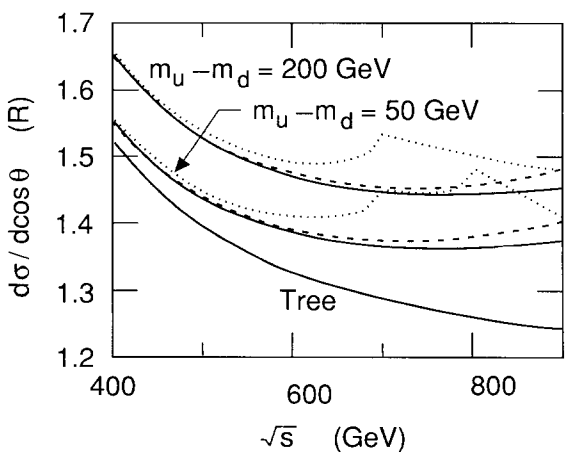

Fig. 12. Effects of fermions with an isospin-breaking mass splitting; $\cos\theta = 0$. Dotted lines: $m_d = 350$ GeV. Dashes: $m_d = 550$ GeV. Solid lines: $m_d = 750$ GeV.

the tree-level amplitudes for W-pair production are unusually small, due to a cancellation of amplitudes. The large size of the corrections is the result of the fact that they do not exhibit the cancellation. On this ground, we would not expect radiative corrections of still higher order to show a further enhancement.

This argument cannot be complete, however, because the size of our correction term, at threshold and above, increases rapidly with the mass of the heavy generation. For example, the residual term (4.8) at very high energies is proportional to m^2. We can understand this dependence by recalling that the production of longitudinal W bosons at high energy is governed by the Equivalence Theorem [27], which states that the production amplitude is equal to that for production of the Goldstone scalars eaten by the W bosons in their mass generation. Indeed, the amplitude for production of scalars through a heavy fermion loop precisely reproduces eq. (4.8), with the prefactor arising from the large fermion–Higgs-Yukawa coupling

$$\frac{\lambda^2}{4\pi} = \frac{1}{4\pi}\left(\frac{m_f}{\langle\phi\rangle}\right)^2 = \frac{\alpha}{2s_\theta^2}\frac{m_f^2}{m_W^2}. \tag{5.1}$$

It has been shown by Chanowitz et al. [28] that quarks with masses above 550 GeV cannot be treated perturbatively, since their Yukawa couplings are sufficiently large to violate tree-level unitarity in four-fermion processes. For such heavy quarks, we must expect large corrections to our calculation, proportional to additional powers of the Yukawa coupling, due to virtual Higgs bosons coupling to the fermion loop. Thus, while our calculations should be trustworthy for small enough quark masses (plausibily, for masses as high as 400 GeV), for higher masses they should be taken only as an indication of the size of the correction to be expected. We should recall, though, that for the main case of interest, $s \ll m^2$, we predict an effect which is independent of mass and so extrapolates smoothly into the high-mass regime.

Heavy scalars exhibit much smaller effects than heavy fermions. Scalars with no mass splitting can acquire a large mass without coupling to the Higgs sector; at low energies these scalars decouple and at high energies they have no strong couplings to longitudinal W's. The only significant corrections for scalars, then, are proportional to the mass-squared splittings within isodoublets. Fig. 13 exhibits this behavior; we see that even for 200 GeV mass splittings in either direction, the vertex effect is small and only the ρ parameter effect is observable. Without a mass splitting, it is impossible to separate the corrected and tree-level curves.

Let us finally discuss the size of the corrections we have found in terms of the expected event samples for future e^+e^- colliders. A design for such a collider which is well matched to the requirements of the physics should provide data samples containing a few thousand events for typical annihilation processes; at $\sqrt{s} = 1$ TeV, such a sample would correspond to a luminosity of 3×10^{33} cm^{-2} sec^{-1} over a running time of a year (3×10^7 sec), for a total integrated luminosity of 9×10^4

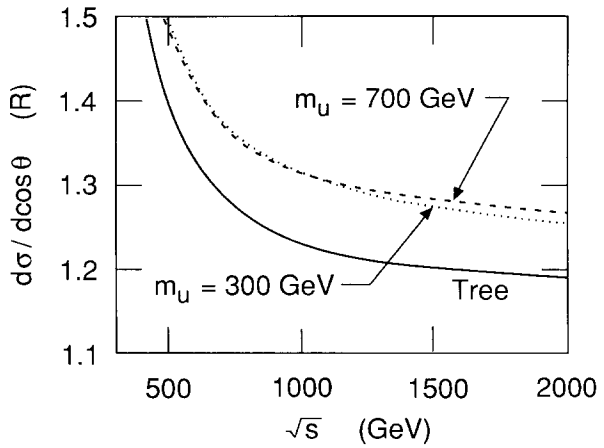

Fig. 13. Effect of a supersymmetric generation of scalar partners; $\cos\theta = 0$, $m_d = 500$ GeV. The upward shift arises almost entirely from the shift in the ρ parameter.

pb^{-1} or 9000 R^{-1}. The heavy fermion corrections could be sought either in the gross form of the distribution in $\cos\theta$ or in the shape of the $\cos\chi$ distribution. The measurement of $\cos\chi$ requires a leptonic decay. Determining the sign of $\cos\theta$ also requires a lepton or a tightly constrained count of charged particles. However, measures of the differential cross section which are symmetric about $\cos\theta = 0$ can be evaluated with essentially the whole sample of W-pair events. Our corrections predict a substantial percentage increase in the cross section except at forward angles, suggesting use of the ratio

$$R_\theta = \int_{|\cos\theta|<0.4} d\cos\theta \frac{d\sigma}{d\cos\theta} \Big/ \int_{|\cos\theta|<0.8} d\cos\theta \frac{d\sigma}{d\cos\theta}. \tag{5.2}$$

This cancels luminosity measurement errors. At $\sqrt{s} = 1$ TeV with a degenerate generation of fermions of mass 750 GeV, using our calculation as an estimate of the effect, we find

$$R_\theta = \begin{cases} 0.305 & \text{heavy fermions}, \\ 0.289 & \text{standard model}. \end{cases} \tag{5.3}$$

For the conditions described at the beginning of this paragraph, the numerator of R_θ corresponds to 11 200 events; these should be accepted with efficiency well above 50%. Thus, the statistical error on R_θ should be about 1.1%, and the effect indicated in eq. (5.3) should be readily observable at nearly 5 standard deviations.

An orthogonal measure of the heavy fermion corrections is

$$R_\chi = \int_{|\cos\chi|<0.6} d\cos\theta\, d\cos\chi \frac{d\sigma}{d\cos\theta\, d\cos\chi} \Big/ \int d\cos\theta\, d\cos\chi \frac{d\sigma}{d\cos\theta\, d\cos\chi}, \quad (5.4)$$

where the denominator includes all events with semileptonic decays and both integrals are taken over $|\cos\theta| < 0.6$. For a heavy generation of fermions of mass 750 GeV and $\sqrt{s} = 1$ TeV, we predict

$$R_\chi = \begin{cases} 0.563 & \text{heavy fermions}, \\ 0.543 & \text{standard model}. \end{cases} \quad (5.5)$$

Roughly 40% of W-pair events will involve one leptonic decay to e or μ, and these events will be readily reconstructed. Thus, for the same conditions, we expect a statistical error on R_χ of 1.4%. At better than 2.5 standard deviations, this can serve to at least independently confirm an effect discovered in the $\cos\theta$ distribution. New fermions of lower mass, but still above threshold, will produce even larger deviations from the standard model predictions, while higher luminosity would lower the statistical errors.

6. Conclusion

Adding a finite, gauge-invariant heavy sector to the standard model gives rise to large effects in $e^+e^- \to W^+W^-$, which we have analyzed in terms of nondecoupling and unitarity delay. Broken global symmetries and large dimensionless parameters are responsible for nondecoupling, while the standard model's gauge cancellations are responsible for unitarity delay. Unitarity delay is most important in the case of longitudinal W's with their kinematicaly enhanced s dependence. Since boson vertex corrections generate the main part of the effect, we are able to glean from this process important information which no fermion production experiment can provide; the three-boson-vertex corrections Σ_{Q+-} and Σ_{3+-} give new and independent contributions from the virtual states. Effects occurring in four-fermion processes (and most easily measured there), including isospin splitting effects on the ρ parameter and running of coupling constants and boson masses, are all summarized in the running electroweak parameters discussed in sect. 3.

At low energy the new contributions are not yet in the asymptotic regime; they disturb the delicate tree-level unitarity cancellation and allow us to probe the nonabelian structure of the standard model's radiative corrections. At higher energies the cancellations are reestablished. For sufficiently heavy fermions or sufficiently split scalars there is also a strong-coupling regime; either strong-coupling effects or our calculated results will be measurable, with a cross-section shift on the order of 0.02 pb.

Appendix A

COMPUTATION OF DIFFERENTIAL CROSS SECTIONS

In this appendix, we give some details of the derivation of the general formulae for the $e^+e^- \to W^+W^-$ differential cross sections ((2.9), (2.13)). These formulae follow straightforwardly from eq. (2.8) by inserting explicit forms for the fermion spinors and the W-bosons' polarization vectors.

To define the electron spinor matrix elements, choose the electron-beam direction as the $\hat{3}$ axis. Then the matrix elements for spinors of definite helicity are given by the simple expression

$$\bar{v}\gamma_\mu u_{R,L} = \sqrt{s}\cdot(\boldsymbol{\varepsilon}_\pm, 0), \quad \text{where} \quad \boldsymbol{\varepsilon}_\pm = \hat{1} \pm i\hat{2}. \tag{A.1}$$

The upper sign refers to the helicity state $e_R^- + e_L^+$, the lower sign to $e_L^- + e_R^+$. The W polarization vectors may be specified more directly as

$$\begin{aligned} \mathscr{E}_T^\alpha &= (\boldsymbol{\epsilon}_T, 0) \quad \text{with} \quad \boldsymbol{q}\cdot\boldsymbol{\epsilon}_T = 0, && \text{for transverse polarization,} \\ \mathscr{E}_L^\alpha &= \frac{1}{m_W}\left(q_0\frac{\boldsymbol{q}}{|\boldsymbol{q}|}, i|\boldsymbol{q}|\right), && \text{for longitudinal polarization.} \end{aligned} \tag{A.2}$$

With these choices, it is straightforward though a bit tedious to work out the explicit values of eq. (2.8) and the t-channel exchange diagram for each polarization state. This calculation yields the following expression for the $e^+e^- \to W^+W^-$ scattering amplitudes between states of definite helicity

$$\mathscr{M} = -ie^2\mathscr{A}, \tag{A.3}$$

where for the various cases of W polarizations:

$$\begin{aligned} \mathscr{A}_{TT} &= A_1\boldsymbol{\varepsilon}_\pm\cdot\hat{q}\boldsymbol{\epsilon}_T^-\cdot\boldsymbol{\epsilon}_T^+ + A_2\left(\hat{3}\cdot\boldsymbol{\epsilon}_T^+\boldsymbol{\varepsilon}_\pm\cdot\boldsymbol{\epsilon}_T^- + \hat{3}\cdot\boldsymbol{\epsilon}_T^-\boldsymbol{\varepsilon}_\pm\cdot\boldsymbol{\epsilon}_T^+\right), \\ \mathscr{A}_{TL} &= A_3\boldsymbol{\varepsilon}_\pm\cdot\boldsymbol{\epsilon}_T^- - A_4\hat{3}\cdot\boldsymbol{\epsilon}_T^-\boldsymbol{\varepsilon}_\pm\cdot\hat{q}, \\ \mathscr{A}_{LT} &= -A_3\boldsymbol{\varepsilon}_\pm\cdot\boldsymbol{\epsilon}_T^+ + A_4\hat{3}\cdot\boldsymbol{\epsilon}_T^+\boldsymbol{\varepsilon}_\pm\cdot\hat{q}, \\ \mathscr{A}_{LL} &= A_5\boldsymbol{\varepsilon}_\pm\cdot\hat{q}, \end{aligned} \tag{A.4}$$

where $\hat{q}$ is a unit vector in the direction of the W^- momentum, $\boldsymbol{\epsilon}_T^\pm$ are the

transverse polarization vectors, and the factors A_i are just those listed in eqs. (2.10) and (2.11).

Squaring this expression and summing over the transverse unit vectors ϵ_T^-, ϵ_T^+ produces precisely the formula (2.9). To obtain eq. (2.13), we require only a small extra piece of analysis. The square of the amplitude for the decay of W^- to $\ell^-\bar{\nu}$, evaluated in the W^- rest frame, is proportional to

$$\epsilon^{i*}[\delta^{ij} - n^i n^j - i\epsilon^{ijk} n^k]\epsilon^j , \tag{A.5}$$

where ϵ is the polarization vector of the W^- and $\boldsymbol{n}$ is a unit vector in the direction of the lepton's momentum as viewed from this frame. We may specify the direction of $\boldsymbol{n}$ in terms of two angles – the angle χ and an azimuthal angle ψ about the $\hat{q}$ axis. We may define χ to be the polar angle between $\boldsymbol{n}$ and $\hat{q}$. Although we can obtain interference terms between different polarizations from this formula, we find it simplest to average over χ; then we may replace in eq. (A.5)

$$n^k \to \hat{q}^k \cos\chi , \qquad n^i n^j \to \hat{q}^i \hat{q}^j \cos^2\chi + \tfrac{1}{2}(\delta^{ij} - \hat{q}^i \hat{q}^j)\sin^2\chi . \tag{A.6}$$

This simplified form of eq. (A.5) may be combined with the squares of the amplitudes (A.4) and summed over W^- polarizations, to yield eq. (2.13) in the narrow-width, on-shell approximation.

Appendix B

EXPLICIT FORMULAE FOR THE W^+W^- FORM FACTORS

In this appendix, we present explicit expressions for the Feynman diagrams of fig. 6, and we convert these expressions to formulae for the one-loop corrected form factors, eq. (3.19). We express these formulae in terms of the one-loop integrals defined by Passarino and Veltman [23], and in terms of a set of reduced Passarino–Veltman functions defined in appendix C.

B.1. HEAVY FERMIONS

We consider first the case of one generation of heavy fermions. To cancel anomalies, we must consider a full generation; our formulae will be written as sums over $f = u_i, d_i, \nu, \ell$ or doublets $d = (u_i, d_i)(\nu, \ell)$, where i runs over 3 colors. When we sum over doublets, the subscripts u and d will denote the up and down components. Q will denote the electric charge of a particle and I_3, Y its isospin and hypercharge: $Q = I_3 + Y$.

The vacuum polarization insertions defined in eq. (3.1) are given in terms of the functions $\boldsymbol{b}_i$, defined in appendix C, by the following expressions [5, 29]

$$16\pi^2 \Pi^p_{QQ}(P^2) = 8 \sum_f Q_f^2 \left[-\tfrac{1}{6}\Delta + \boldsymbol{b}_3\left(P^2, m_f^2, m_f^2\right)\right],$$

$$16\pi^2 \Pi^p_{3Q}(P^2) = 4 \sum_f (QI_3)_f \left[-\tfrac{1}{6}\Delta + \boldsymbol{b}_3\left(P^2, m_f^2, m_f^2\right)\right],$$

$$16\pi^2 \Pi_{33}(P^2) = 2 \sum_f (I_3)_f^2 \Big[2P^2 \left(-\tfrac{1}{6}\Delta + \boldsymbol{b}_3\left(P^2, m_f^2, m_f^2\right)\right)$$

$$- m_f^2 \left(\Delta + \boldsymbol{b}_0\left(P^2, m_f^2, m_f^2\right)\right)\Big],$$

$$16\pi^2 \Pi_{11}(P^2) = \sum_d \Big[2P^2 \left(-\tfrac{1}{6}\Delta + \boldsymbol{b}_3\left(P^2, m_u^2, m_d^2\right)\right) - \tfrac{1}{2}\left(m_u^2 + m_d^2\right)\Delta$$

$$+ m_d^2 \boldsymbol{b}_1\left(P^2, m_d^2, m_u^2\right) + m_u^2 \boldsymbol{b}_1\left(P^2, m_u^2, m_d^2\right)\Big]. \quad \text{(B.1)}$$

Here, Δ is the divergence of dimensional regularization, $\Delta = \pi^{-(2-d/2)}\Gamma(2 - \frac{1}{2}d) \sim 1/(2 - \frac{1}{2}d) - \gamma - \ln\pi$. An arbitrary mass parameter $\ln m_R^2$, arising from coupling-constant dimensions and serving to eliminate dimensionful logarithms, follows Δ and cancels out along with it. From these formulae, we can immediately assemble expressions for the heavy particle contributions to the running coupling constants, the running Z mass, and the wave function factor ξ. For the running couplings,

$$\frac{1}{e_*^2(P^2)} - \frac{1}{e_*^2(\mu^2)} = -\sum_f \left[\frac{8}{16\pi^2} Q_f^2 \left(\boldsymbol{b}_3\left(P^2, m_f^2, m_f^2\right) - \boldsymbol{b}_3\left(\mu^2, m_f^2, m_f^2\right)\right)\right],$$

$$\frac{1}{g_*^2(P^2)} - \frac{1}{g_*^2(\mu^2)} = -\sum_f \left[\frac{4}{16\pi^2} (QI_3)_f \left(\boldsymbol{b}_3\left(P^2, m_f^2, m_f^2\right) - \boldsymbol{b}_3\left(\mu^2, m_f^2, m_f^2\right)\right)\right]. \quad \text{(B.2)}$$

The factor ξ becomes

$$(\xi - 1) = \frac{g_*^2}{16\pi^2} \sum_d \Big[\frac{\partial}{\partial P^2} \left\{ 2P^2 \boldsymbol{b}_3\left(P^2, m_u^2, m_d^2\right) + m_u^2 \boldsymbol{b}_1\left(P^2, m_u^2, m_d^2\right)\right.$$

$$\left. + m_d^2 \boldsymbol{b}_1\left(P^2, m_d^2, m_u^2\right)\right\}\Big|_{P^2 = -m_W^2}$$

$$- 4\left\{ \tfrac{1}{2}\left(\tfrac{1}{2} + Y\right) \boldsymbol{b}_3\left(P^2, m_u^2, m_u^2\right) + \tfrac{1}{2}\left(\tfrac{1}{2} - Y\right) \boldsymbol{b}_3\left(P^2, m_d^2, m_d^2\right)\right\}\Big]. \quad \text{(B.3)}$$

We require the running Z mass in the particular form in which it appears in eq. (3.17); for a generation of fermion doublets this is

$$M_{Z_*}^2 - m_Z^2$$

$$= \frac{g_*^2}{16\pi^2 c_*^2} \sum_f \Big[8Q_f^2 m_Z^2 \big[b_3(P^2) - b_3(-m_Z^2) \big]$$

$$+ 4(I_3 Q)_f \Big\{ \big[P^2 + m_Z^2(1 - 2s_*^2) \big] b_3(P^2) + 2m_Z^2 s_*^2 b_3(-m_Z^2) \Big\}$$

$$- P^2 b_3(P^2) - m_Z^2 b_3(-m_Z^2) + \tfrac{1}{2} m_f^2 \big[b_0(P^2) - b_0(-m_Z^2) \big] \Big] . \quad \text{(B.4)}$$

The computation of the vertex diagrams, fig. 6b, is less straightforward. After performing the Dirac algebra, one must gather terms together into the Lorentz structures given in eq. (2.1), ignoring terms proportional to the electron mass and using the trick given in appendix A of ref. [18] to eliminate additional structures. After this rearrangement, the coefficients of the structures T_4, T_6 and T_7 disappear as required. Evaluating the integrals using dimensional regularization, we find additional finite terms of the form

$$\Delta\big(2 - \tfrac{1}{2}d\big) \to 1 , \quad \text{(B.5)}$$

arising from fermion traces. It is essential to keep these terms in order to obtain the unitarity cancellation in the one-loop corrections. The final result can be written as follows

$$\Sigma_{3+-} = \tfrac{1}{2} \sum_{\text{doublets}} \big[(I_3)_d H\big(P^2, m_u^2, m_d^2\big) - (I_3)_u \tilde{H}\big(P^2, m_d^2, m_u^2\big) \big]$$

$$\Sigma_{Q+-} = \tfrac{1}{2} \sum_{\text{doublets}} \big[Q_d \big[H\big(P^2, m_u^2, m_d^2\big) - G\big(P^2, m_u^2, m_d^2\big) \big]$$

$$- Q_u \big[\tilde{H}\big(P^2, m_d^2, m_u^2\big) - \tilde{G}\big(P^2, m_d^2, m_u^2\big) \big] \big] , \quad \text{(B.6)}$$

where $H = \sum_i H^{(i)} T_i$ and $\tilde{H} = H - 2H^{(4)}T_4 - 2H^{(5)}T_5$, i.e. T_4 and T_5 reverse sign,

and similarly with G. Finally, in terms of Passarino–Veltman integrals

$$16\pi^2 G(P^2, m_1^2, m_2^2) = (T_0 - T_3 - T_5)\frac{m_1^2}{m_R^2}(c_2 - c_3),$$

$$\begin{aligned} 16\pi^2 H(P^2, m_1^2, m_2^2) = T_0 &\left(\tfrac{2}{3}(1-\Delta) + c_0 + c_1 - \frac{m_W^2}{m_R^2}(c_4 - c_5) - \frac{s}{m_R^2}(c_6 + c_7) \right) \\ &- 4T_2 \frac{m_W^2}{m_R^2} c_7 \\ &+ T_3 \left(c_0 - 3c_1 - \frac{m_W^2}{m_R^2}(2c_3 - 5c_4 + 3c_5) + \frac{s}{m_R^2}(c_6 + 3c_7) \right) \\ &+ T_5 \left(-c_0 + 3c_1 - \frac{m_W^2}{m_R^2}(c_4 - c_5) + \frac{s}{m_R^2}(c_6 - c_7) \right); \end{aligned} \quad \text{(B.7)}$$

the c_i have arguments (P^2, m_1^2, m_2^2).

B.2. HEAVY SCALARS

We now consider a hypothetical heavy scalar doublet $\Phi = (\phi_u, \phi_d)$ with SU(2) × U(1) quantum numbers $I_3 = \pm \frac{1}{2}$, $Q = (Q_u, Q_d)$, masses (m_u, m_d), and vanishing vacuum expectation value. We obtain vertex corrections

$$\begin{aligned} \Sigma_{Q+-} = \frac{1}{16\pi^2} &\left[Q_u \left(\left(\tfrac{1}{6}\Delta - c_1\right) T_0 - 2\frac{m_W^2}{m_R^2} c_7 T_2 + (3c_1 - c_0) T_3 \right) (P^2, m_d^2, m_u^2) \right. \\ &\left. - Q_d \left(\left(\tfrac{1}{6}\Delta - c_1\right) T_0 - 2\frac{m_W^2}{m_R^2} c_7 T_2 + (3c_1 - c_0) T_3 \right) (P^2, m_u^2, m_d^2) \right], \end{aligned}$$

$$\begin{aligned} \Sigma_{3+-} = \frac{\frac{1}{2}}{16\pi^2} &\left[\left(\left(\tfrac{1}{6}\Delta - c_1\right) T_0 - 2\frac{m_W^2}{m_R^2} c_7 T_2 + (3c_1 - c_0) T_3 \right) (P^2, m_u^2, m_d^2) \right. \\ &\left. + \left(\left(\tfrac{1}{6}\Delta - c_1\right) T_0 - 2\frac{m_W^2}{m_R^2} c_7 T_2 + (3c_1 - c_0) T_3 \right) (P^2, m_d^2, m_u^2) \right], \end{aligned} \quad \text{(B.8)}$$

and two-point corrections [29, 30]

$$\Pi^p_{QQ} = -\frac{1}{16\pi^2}\left[Q_u^2\left(\tfrac{1}{3}\Delta + 4b_3 + b_0\right)\left(P^2, m_u^2, m_u^2\right)\right.$$

$$\left. + Q_d^2\left(\tfrac{1}{3}\Delta + 4b_3 + b_0\right)\left(P^2, m_d^2, m_d^2\right)\right],$$

$$\Pi^p_{3Q} = -\frac{1}{2}\frac{1}{16\pi^2}\left[Q_u\left(\tfrac{1}{3}\Delta + 4b_3 + b_0\right)\left(P^2, m_u^2, m_u^2\right)\right.$$

$$\left. - Q_d\left(\tfrac{1}{3}\Delta + 4b_3 + b_0\right)\left(P^2, m_d^2, m_d^2\right)\right],$$

$$\Pi_{33} = -\frac{1}{16\pi^2}\frac{P^2}{4}\left[\frac{2}{3}\Delta + (4b_3 + b_0)\left(P^2, m_u^2, m_u^2\right) + (4b_3 + b_0)\left(P^2, m_d^2, m_d^2\right)\right],$$

$$\Pi_{11} = -\frac{1}{2}\frac{1}{16\pi^2}\left[P^2\left(\tfrac{1}{3}\Delta + 4b_3 + b_0\right)\left(P^2, m_u^2, m_d^2\right)\right.$$

$$\left. + \left(m_d^2 - m_u^2\right)\left[b_1\left(P^2, m_d^2, m_u^2\right) - b_1\left(P^2, m_u^2, m_d^2\right)\right]\right]. \qquad \text{(B.9)}$$

For the case of a full generation of superpartners, we can sum over sleptons and squarks.

Appendix C

REDUCED PASSARINO–VELTMAN FUNCTIONS

All higher Passarino–Veltman functions may be uniquely decomposed into linear combinations of the scalar integrals B_0 and C_0, for which closed-form expressions are known [23, 34]. The decomposition algorithm has been implemented in an algebraic manipulation program [26]; for purposes of asymptotic analysis, however, we have found it convenient to define reduced Passarino–Veltman functions representing finite, dimensionless parts of two- and three-point one-loop integrals. All of these functions include an arbitrary mass scale m_R, which cancels out of all physical results. For the two-point functions, it is straightforward to determine the asymptotic forms of these functions. For the three-point functions, the asymptotic analysis requires some effort, and so we have catalogued the required formulae.

The functions $\boldsymbol{b}_i(P^2, m_1^2, m_2^2)$ which appear in appendix C are defined as follows

$$[\boldsymbol{b}_0, \boldsymbol{b}_1, \boldsymbol{b}_3] = \int_0^1 \mathrm{d}x \log\left(\left[xm_1^2 + (1-x)m_2^2 + x(1-x)P^2 - i\epsilon\right]/m_R^2\right) \times [-1, x, x(1-x)]\,. \tag{C.1}$$

These functions are related to the corresponding Passarino–Veltman integrals [23] by

$$\begin{aligned} B_0(m_2, m_1) &= \boldsymbol{b}_0(m_1, m_2) + \left(\Delta - \ln m_R^2\right), \\ B_1(m_2, m_1) &= \boldsymbol{b}_1(m_1, m_2) - \tfrac{1}{2}\left(\Delta - \ln m_R^2\right), \\ B_3(m_2, m_1) &= \boldsymbol{b}_3(m_1, m_2) - \tfrac{1}{6}\left(\Delta - \ln m_R^2\right), \end{aligned} \tag{C.2}$$

with $B_3 = B_{21} + B_1$; B_3 and B_0 are symmetric in m_1^2, m_2^2.

Passarino and Veltman's C functions are defined by

$$\begin{aligned} &C_{0,\mu,\mu\nu,\mu\nu\rho}\left(q^2, \bar{q}^2, P^2, m_1^2, m_2^2, m_3^2\right) \\ &\quad \equiv \int \frac{\mathrm{d}^d k}{i\pi^2} \frac{\{1, k_\mu, k_\mu k_\nu, k_\mu k_\nu k_\rho\}}{\left(k^2 + m_1^2\right)\left[(k+q)^2 + m_2^2\right]\left[(k+P)^2 + m_3^2\right]}\,, \end{aligned} \tag{C.3}$$

and can be written in terms of form factors;

$$\begin{aligned} C_\mu &= \bar{q}_\mu C_{11} + q_\mu C_{12}\,, \\ C_{\mu\nu} &= \bar{q}_\mu \bar{q}_\nu C_{21} + q_\mu q_\nu C_{22} + \{q\bar{q}\}_{\mu\nu} C_{23} + \delta_{\mu\nu} C_{24}\,, \\ C_{\mu\nu\rho} &= \bar{q}_\mu \bar{q}_\nu \bar{q}_\rho C_{31} + q_\mu q_\nu q_\rho C_{32} \\ &\quad + \{q\bar{q}q\}_{\mu\nu\rho} C_{33} + \{\bar{q}qq\}_{\mu\nu\rho} C_{34} \\ &\quad + \{\bar{q}\delta\}_{\mu\nu\rho} C_{35} + \{q\delta\}_{\mu\nu\rho} C_{36}\,, \end{aligned} \tag{C.4}$$

with braces summing over distinct permutations and $P = q + \bar{q}$ always.

In the present case we may set $m_1^2 = m_3^2 \to m_2^2$ and $m_2^2 \to m_1^2$; then we define the reduced Passarino–Veltman functions $\boldsymbol{c}_i(P^2, m_1^2, m_2^2)$ in terms of the denominator

$$D = zm_1^2 + (1-z)m_2^2 - z(1-z)m_W^2 + xyP^2 - i\epsilon\,, \tag{C.5}$$

as follows

$$[c_0, c_1] = \int dx\, dy\, dz\, \delta(x+y+z-1)\log\left(D/m_R^2\right)[1, z],$$

$$[c_2, c_3, c_4, c_5, c_6, c_7] = \int dx\, dy\, dz\, \delta(x+y+z-1)\left(m_R^2/D\right) \times \left[1, z, z^2, z^3, xy, xyz\right]. \tag{C.6}$$

Note that

$$[c_6, c_7] = \frac{m_R^2}{s}\left[-\tfrac{1}{2}, -\tfrac{1}{6}\right] + \frac{m_2^2}{s}[c_2, c_3] + \frac{\left(m_1^2 - m_2^2 - m_W^2\right)}{s}[c_3, c_4] + \frac{m_W^2}{s}[c_4, c_5]. \tag{C.7}$$

These functions are related to the corresponding Passarino–Veltman integrals by

$$m_R^2 C_0 = c_2, \qquad m_R^2 C_{11,12} = -\tfrac{1}{2}(c_2 \pm c_3),$$

$$m_R^2 C_{21} = \tfrac{1}{2}(c_2 + c_4) - c_6,$$

$$m_R^2 C_{22} = \tfrac{1}{2}(c_2 + c_4) - c_3 - c_6,$$

$$m_R^2 C_{23} = \tfrac{1}{2}(c_2 - c_3) - c_6,$$

$$m_R^2 C_{31} = -\tfrac{1}{2}(c_2 + c_5) + \tfrac{3}{2}(c_6 + c_7),$$

$$m_R^2 C_{32} = -\tfrac{1}{2}(c_2 - 3c_3 + 3c_4 - c_5) + \tfrac{3}{2}(c_6 - c_7),$$

$$m_R^2 C_{33} = -\tfrac{1}{2}(c_2 - c_3) + \tfrac{3}{2}c_6 + \tfrac{1}{2}c_7,$$

$$m_R^2 C_{34} = -\tfrac{1}{2}(c_2 + c_4) + c_3 + \tfrac{3}{2}c_6 - \tfrac{1}{2}c_7,$$

$$C_{24} = -\tfrac{1}{2}c_0 + \tfrac{1}{4}\left(\Delta - \ln m_R^2\right),$$

$$C_{35} = \tfrac{1}{4}(c_0 + c_1) - \tfrac{1}{6}\left(\Delta - \ln m_R^2\right),$$

$$C_{36} = \tfrac{1}{4}(c_0 - c_1) - \tfrac{1}{12}\left(\Delta - \ln m_R^2\right), \tag{C.8}$$

where

$$C_{ij} = C_{ij}\left(-m_W^2, -m_W^2, P^2, m_2^2, m_1^2, m_2^2\right),$$

$$c_i = c_i\left(P^2, m_1^2, m_2^2\right). \tag{C.9}$$

We reduce the integrations over three Feynman parameters to one-parameter integrations for numerical analysis and asymptotic expression.

$$[c_0, c_1] = \int_0^1 dz \left\{ (1-z)\left(\ln\frac{A}{m_R^2} - 2 - i\pi\theta(-A) \right) + |R(z,s)|^{1/2} K(z) \right\} [1, z]$$

$$[c_2, c_3, c_4, c_5] = \int_0^1 dz \, \frac{2m_R^2}{s} |R(z,s)|^{-1/2} Q(z) K(z) [1, z, z^2, z^3], \tag{C.10}$$

where we define

$$A(z) = z m_1^2 + (1-z) m_2^2 - z(1-z) m_W^2, \tag{C.11}$$

$$R(z,s) = \frac{4A}{s} - (1-z)^2, \tag{C.12}$$

$$Q(z) = \begin{cases} 1 & \text{for} \quad z > z_+, \\ -1 & \text{for} \quad z < z_+, \end{cases} \tag{C.13}$$

$$K(z) = \begin{cases} 2\arctan\left[(1-z)|R(z,s)|^{-1/2}\right], & \text{for} \quad z_+ < z \leqslant 1, \\ \ln\left[\dfrac{(1-z) + |R(z,s)|^{1/2}}{(1-z) - |R(z,s)|^{1/2}} \right] - i\pi\theta(A), & \text{for} \quad 0 \leqslant z < z_+, \end{cases} \tag{C.14}$$

and z_+, a solution for $R(z,s) = 0$, is given by

$$z_+ = \frac{s + 2\left(m_1^2 - m_2^2 - m_W^2\right)}{s - 4m_W^2}$$

$$- \frac{2}{s - 4m_W^2} \left[m_1^2 s + \left(m_1^2 - m_2^2\right)^2 - 2m_W^2\left(m_1^2 + m_2^2\right) + m_W^4 \right]^{1/2}. \tag{C.15}$$

For present purposes, we may disregard the imaginary parts.

For large and small values of s, the functions c_i take the following asymptotic forms. We always assume that the mass difference between m_1 and m_2 is small and

set $\Delta m^2 = m_1^2 - m_2^2$, $m^2 = \frac{1}{2}(m_1^2 + m_2^2)$, with $\Delta m^2 \ll m^2$. Then for $m_W^2 \ll s \ll m^2$

$$c_0 = \tfrac{1}{2}\ln\frac{s}{m_R^2} - \frac{1}{12}\frac{\Delta m^2}{m^2} - \frac{1}{24}\frac{s}{m^2},$$

$$c_1 = \tfrac{1}{6}\ln\frac{s}{m_R^2} - \frac{1}{120}\frac{s}{m^2},$$

$$c_2 = \frac{m_R^2}{m^2}\left[\tfrac{1}{2} + \frac{1}{12}\frac{\Delta m^2}{m^2} + \frac{1}{24}\frac{s}{m^2}\right],$$

$$c_3 = \frac{m_R^2}{m^2}\left[\tfrac{1}{6} + \frac{1}{120}\frac{s}{m^2}\right],$$

$$c_4 = \frac{m_R^2}{m^2}\left[\tfrac{1}{12} - \frac{1}{120}\frac{\Delta m^2}{m^2} + \frac{1}{360}\frac{s}{m^2}\right],$$

$$c_5 = \frac{m_R^2}{m^2}\left[\tfrac{1}{20} - \frac{1}{120}\frac{\Delta m^2}{m^2} + \frac{1}{840}\frac{s}{m^2}\right],$$

$$c_6 = \frac{m_R^2}{m^2}\left[\tfrac{1}{24} + \frac{1}{80}\frac{\Delta m^2}{m^2} + \frac{1}{180}\frac{s}{m^2}\right],$$

$$c_7 = \frac{m_R^2}{m^2}\left[\tfrac{1}{120} + \frac{1}{720}\frac{\Delta m^2}{m^2} + \frac{1}{1260}\frac{s}{m^2}\right]. \tag{C.16}$$

When $s \gg m^2$, dropping $\Delta m^2/m^2$ and nonasymptotic terms

$$c_0 = \tfrac{1}{2}\ln\frac{s}{m_R^2} - \tfrac{3}{2} - \frac{m^2}{s}\left[\tfrac{1}{2}\left[\ln^2\left(\frac{s}{m^2}\right) - \pi^2\right] + \ln\left(\frac{s}{m^2}\right) + 1\right],$$

$$c_1 = \tfrac{1}{6}\ln\left(\frac{s}{m_R^2}\right) - \tfrac{11}{18} - \frac{m^2}{s}\left[\tfrac{1}{2}\left[\ln^2\left(\frac{s}{m^2}\right) - \pi^2\right] - \ln\left(\frac{s}{m^2}\right) + 3\right],$$

$$\frac{s}{m_R^2}c_2 = -\tfrac{1}{2}\left[\ln^2\left(\frac{s}{m^2}\right) - \pi^2\right] + \frac{m^2}{s}\left[2\ln\frac{s}{m^2}\right],$$

$$\frac{s}{m_R^2}c_3 = -\tfrac{1}{2}\left[\ln^2\left(\frac{s}{m^2}\right) - \pi^2\right] + 2\ln\frac{s}{m^2} - 4 + \frac{m^2}{s}\left[-2\ln\left(\frac{s}{m^2}\right) - 4\right],$$

$$\frac{s}{m_R^2}c_4 = -\tfrac{1}{2}\left[\ln^2\left(\frac{s}{m^2}\right) - \pi^2\right] + 3\ln\left(\frac{s}{m^2}\right) - 7$$

$$+ \frac{m^2}{s}\left[-\left[\ln^2\left(\frac{s}{m^2}\right) - \pi^2\right] - 4\ln\left(\frac{s}{m^2}\right) - 6\right],$$

$$\frac{s}{m_R^2}c_5 = -\tfrac{1}{2}\left[\ln^2\left(\frac{s}{m^2}\right) - \pi^2\right] + \tfrac{11}{3}\ln\left(\frac{s}{m^2}\right) - \tfrac{85}{9}$$

$$+ \frac{m^2}{s}\left[-3\left[\ln^2\left(\frac{s}{m^2}\right) - \pi^2\right] - 18\right],$$

$$\frac{s}{m_R^2}c_6 = -\tfrac{1}{2} + \frac{m^2}{s}\left[-\tfrac{1}{2}\left[\ln^2\left(\frac{s}{m^2}\right) - \pi^2\right]\right],$$

$$\frac{s}{m_R^2}c_7 = -\tfrac{1}{6} + \frac{m^2}{s}\left[-\tfrac{1}{2}\left[\ln^2\left(\frac{s}{m^2}\right) - \pi^2\right] + 2\ln\left(\frac{s}{m^2}\right) - 4\right]. \qquad \text{(C.17)}$$

We are grateful to Gary Feldman and Rick van Kooten for discussions of the actual measurement of W-pair production at TeV energies. We also thank Dallas Kennedy, Helen Quinn, Robin Stuart, and Puru Voruganti for their useful advice. S.B.S. is grateful to acknowledge that his work is supported by a National Science Foundation Graduate fellowship.

References

[1] M. Veltman, Phys. Lett. B91 (1980) 95
[2] W.J. Marciano and A. Sirlin, Phys. Rev. D29 (1984) 945; D31 (1985) 213; Phys. Rev. Lett. 46 (1981) 163
[3] A. Sirlin, Phys. Rev. D22 (1980) 971
[4] B.W. Lynn and R.G. Stuart, Nucl. Phys. B253 (1985) 216
[5] D.C. Kennedy and B.W. Lynn, SLAC-PUB-4039 (1988)
[6] B.W. Lynn, M.E. Peskin and R.G. Stuart, *in* Tests of electroweak theories, eds. B.W. Lynn, C. Verzegnassi (World Scientific, Singapore, 1986)
[7] T. Applequist and J. Carazzone, Phys. Rev. D11 (1975) 2856
[8] J. Collins, F. Wilczek and A. Zee, Phys. Rev. D18 (1978) 242
[9] W. Alles, Ch. Boyer and A. Buras, Nucl. Phys. B119 (1977) 125
[10] O.P. Sushkov, V.V. Flambaum and I.B. Khriplovich, Sov. J. Nucl. Phys. 20 (1975) 537
[11] J.M. Cornwall, D.N. Levin and G. Tiktopoulos, Phys. Rev. D10 (1974) 1145. (E) D11 (1975) 972
[12] M. Kuroda, F.M. Renard and D. Schildknecht, Phys. Lett. B183 (1987) 366
[13] M. Lemoine and M. Veltman, Nucl. Phys. B164 (1980) 445
[14] R. Philippe, Phys. Rev. D26 (1982) 1588
[15] B. Grzadkowski and Z. Hioki, Phys. Lett. B197 (1987) 213
[16] P. Kalyniak and M.K. Sundaresan, Carleton Univ. preprint 87-0800 (1987)
[17] M. Bohm, A. Denner, T. Sack, W. Beenakker, F. Berends and H. Kuijf, Nucl. Phys. B304 (1988) 463

[18] K. Hagiwara, R.D. Peccei, D. Zeppenfeld and K. Hikasa, Nucl. Phys. B262 (1987) 233
[19] S. Selipsky and B.W. Lynn, in preparation
[20] D.C. Kennedy, B.W. Lynn and C.J.-C. Im, SLAC-PUB-4128 (1988)
[21] M. Veltman, Nucl. Phys. B123 (1977) 89
[22] U. Amaldi, A. Bohm, L.S. Durkin, P. Langacker, A.K. Mann, W.J. Marciano, A. Sirlin and H.H. Williams, Phys. Rev. D36 (1987) 1385
[23] G. Passarino and M. Veltman, Nucl. Phys. B160 (1979) 151
[24] G. 't Hooft and M. Veltman, Nucl. Phys. B153 (1979) 365
[25] B.W. Lynn, Ph.D. thesis, Columbia University (1982); University Microfilms
[26] R.G. Stuart, Max Planck Institute preprint MPI-PAE/PTh 85/87 (1987)
[27] M.S. Chanowitz and M.K. Gaillard, Nucl. Phys. B261 (1985) 379;
B.W. Lee, C. Quigg and H. Thacker, Phys. Rev. D16 (1977) 1519;
J.M. Cornwall, D.N. Levin and G. Tiktopolous, ref. [11];
C.E. Vayonakis, Lett. Nuovo Cim. 17 (1976) 383;
G.J. Gounaris, R. Kogerler and H. Neufeld, Phys. Rev. D34 (1986) 3257
[28] M.S. Chanowitz, M.A. Furman and I. Hinchliffe, Nucl. Phys. B153 (1979) 402
[29] R.G. Stuart, D. Phil. thesis, Oxford University (1985)
[30] B.W. Lynn, SLAC-PUB-3358 (1984)